1. Studies of signal and background separation using calorimeter clusters

In this section, we study different jet substructure variables and compare their ability to separate the signal and the background for different detector sizes using calorimeter clusters.

Figures 1–3 show the ROC curves of three variables, $c_2^{(1)}$ [**?**] , τ_{21} [**?**], and τ_{32} [**?**], respectively. Three different cell sizes of the HCAL are compared for four collision energies. For different cell sizes with the same signal efficiency, the one with the highest background rejection rate, namely (1-background efficiency), has the highest separate power.

In Figure 1 for the variable $c_2^{(1)}$, the ROC curves of the three detector cell sizes are close to each other for each collision energy. Therefore, this variable is not sensitive to the detector cell size.

For the τ_{21} variable in Figure 2, at 5 TeV, the smallest detector size (1×1 cm) can separate the background from the signal well. However, this is not the usual case as the ROC curves nearly merge together at higher collision energy. In addition, the detector with the bigger size tends to have higher separation power than the smaller detector size in 20 and 40 TeV collision energy.

Figure 3 shows the variable τ_{32}, where the smallest detector size has the best separation power for all collision energies.

In conclusion, in all the cases of energy and detector size, the variable $c_2^{(1)}$ has the best separation power compared to the other two variables. In addition, the variable τ_{32} follows the expectation that smaller detector size has better separation power.

2. Studies of signal and background separation using calorimeter hit cut at 0.5GeV

3. Studies of signal and background separation using calorimeter hit cut at 0.25GeV

4. Studies of signal and background separation using calorimeter hit compare cut at 0.25GeV and cut at 0.5GeV

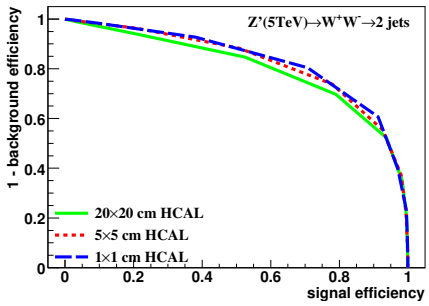

(a) 5 TeV in cluster

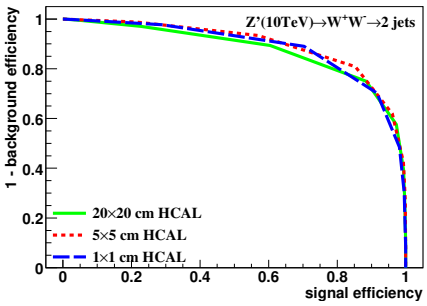

(b) 10 TeV in cluster

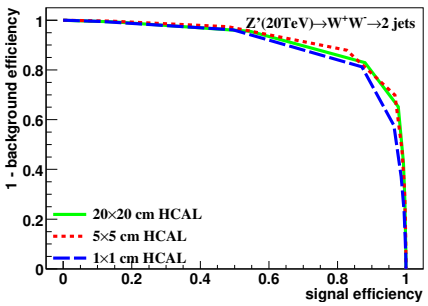

(c) 20 TeV in cluster

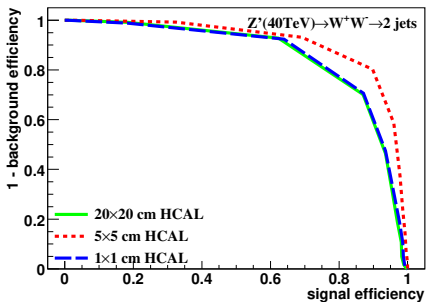

(d) 40 TeV in cluster

Figure 1: Signal efficiency versus background rejection rate using $c_2^{(1)}$.The energies of collision at (a)5, (b)10, (c)20, (d)40TeV are shown here. In each picture, the three ROC curves correspond to different detector sizes.

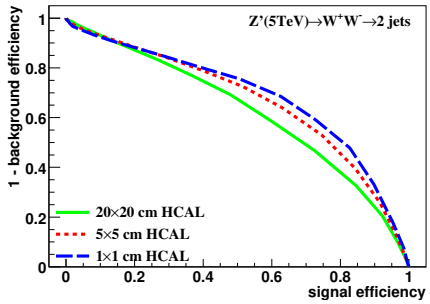

(a) 5 TeV in cluster

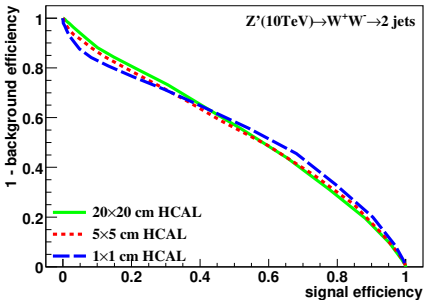

(b) 10 TeV in cluster

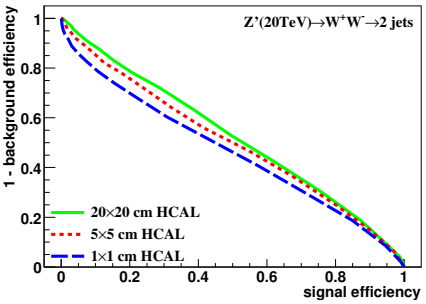

(c) 20 TeV in cluster

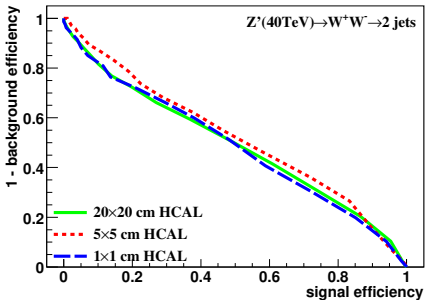

(d) 40 TeV in cluster

Figure 2: Signal efficiency versus background rejection rate using τ_{21}.The energies of collision at (a)5, (b)10, (c)20, (d)40TeV are shown here. In each picture, the three ROC curves correspond to different detector sizes.

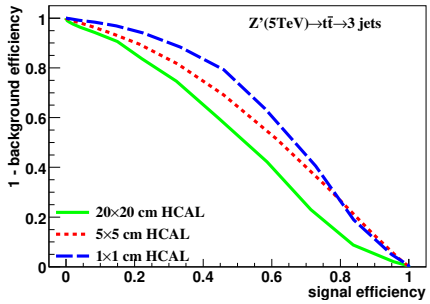

(a) 5 TeV in cluster

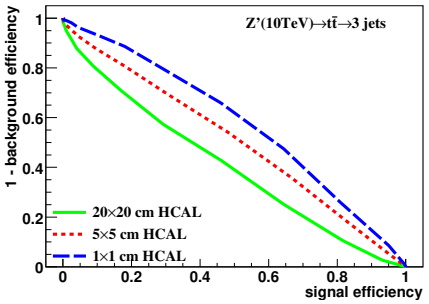

(b) 10 TeV in cluster

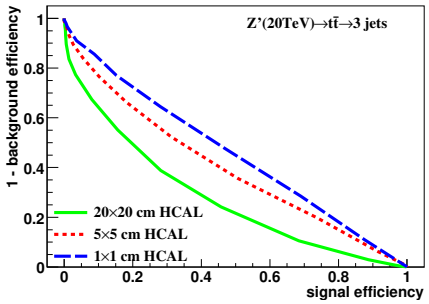

(c) 20 TeV in cluster

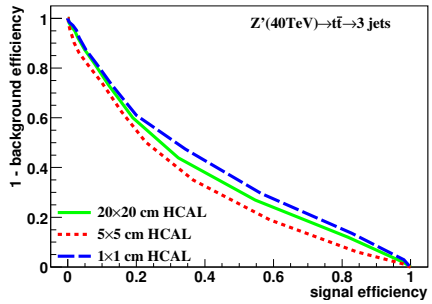

(d) 40 TeV in cluster

Figure 3: Signal efficiency versus background rejection rate using τ_{32}.The energies of collision at (a)5, (b)10, (c)20, (d)40TeV are shown here. In each picture, the three ROC curves correspond to different detector sizes.

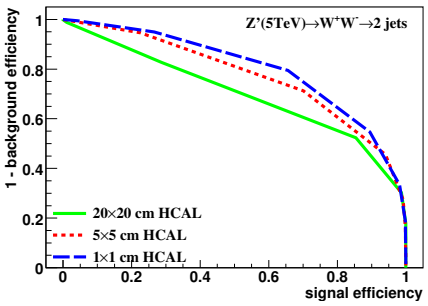

(a) 5 TeV rawhit cut at 0.5GeV

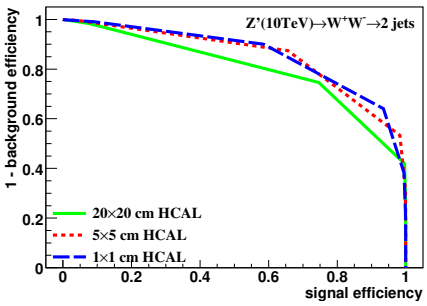

(b) 10 TeV rawhit cut at 0.5GeV

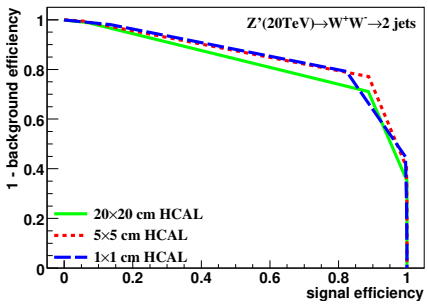

(c) 20 TeV rawhit cut at 0.5GeV

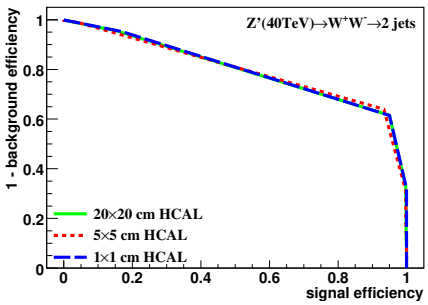

(d) 40 TeV rawhit cut at 0.5GeV

Figure 4: Signal efficiency versus background rejection rate using $c_2^{(1)}$.The energies of collision at (a)5, (b)10, (c)20, (d)40TeV are shown here. In each picture, the three ROC curves correspond to different detector sizes.

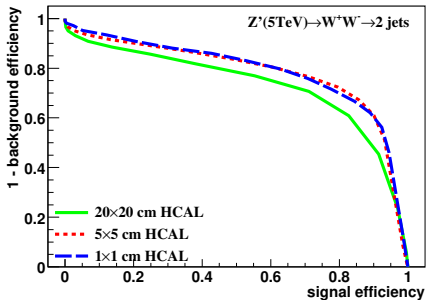

(a) 5 TeV rawhit cut at 0.5GeV

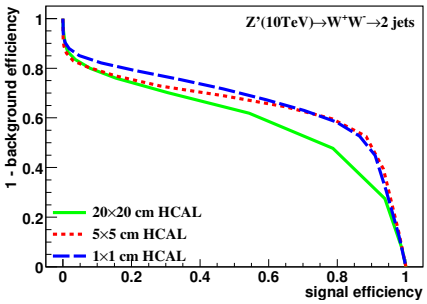

(b) 10 TeV rawhit cut at 0.5GeV

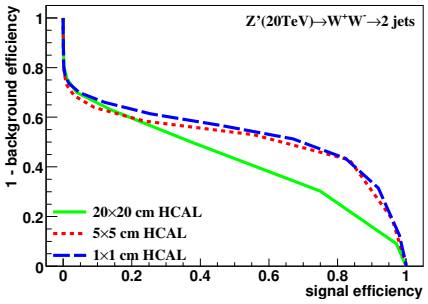

(c) 20 TeV rawhit cut at 0.5GeV

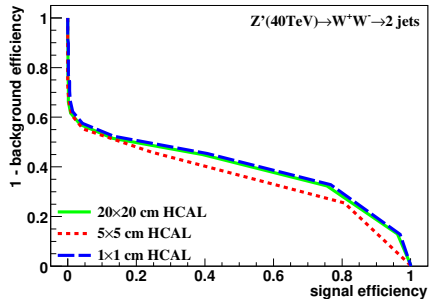

(d) 40 TeV rawhit cut at 0.5GeV

Figure 5: Signal efficiency versus background rejection rate using τ_{21}.The energies of collision at (a)5, (b)10, (c)20, (d)40TeV are shown here. In each picture, the three ROC curves correspond to different detector sizes.

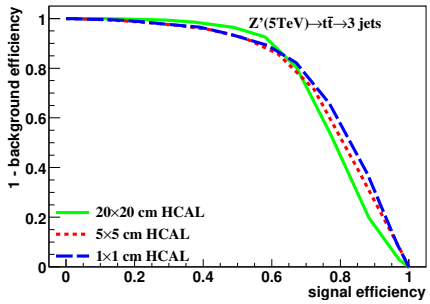

(a) 5 TeV rawhit cut at 0.5GeV

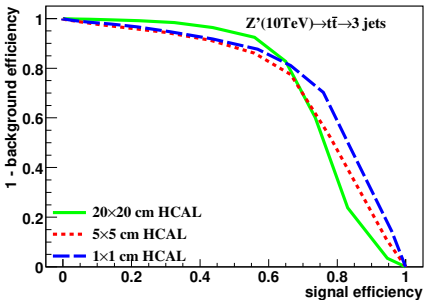

(b) 10 TeV rawhit cut at 0.5GeV

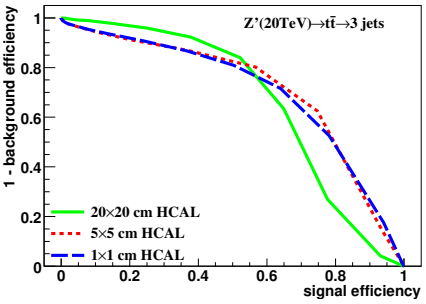

(c) 20 TeV rawhit cut at 0.5GeV

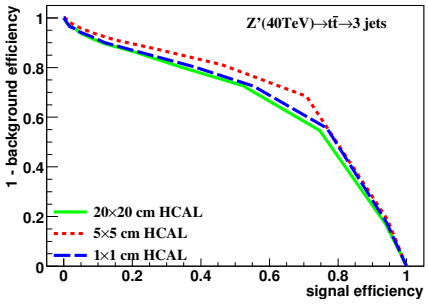

(d) 40 TeV rawhit cut at 0.5GeV

Figure 6: Signal efficiency versus background rejection rate using τ_{32}.The energies of collision at (a)5, (b)10, (c)20, (d)40TeV are shown here. In each picture, the three ROC curves correspond to different detector sizes.

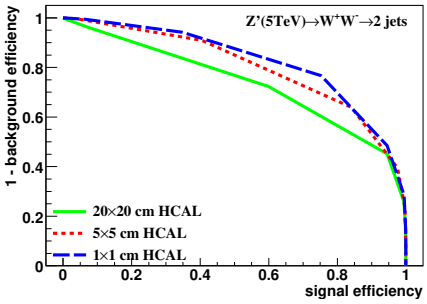

(a) 5 TeV rawhit cut at 0.25GeV

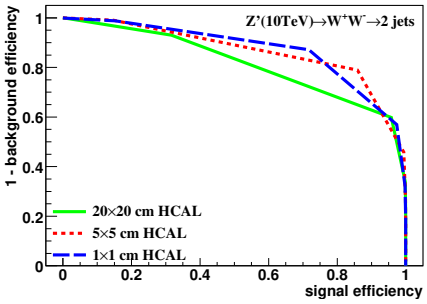

(b) 10 TeV rawhit cut at 0.25GeV

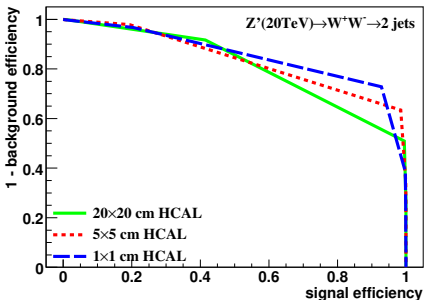

(c) 20 TeV rawhit cut at 0.25GeV

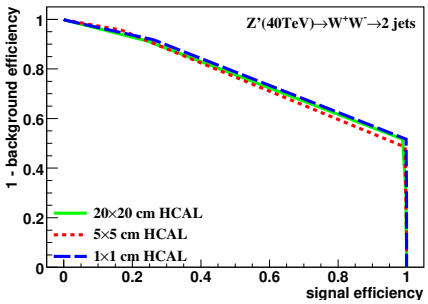

(d) 40 TeV rawhit cut at 0.25GeV

Figure 7: Signal efficiency versus background rejection rate using $c_2^{(1)}$.The energies of collision at (a)5, (b)10, (c)20, (d)40TeV are shown here. In each picture, the three ROC curves correspond to different detector sizes.

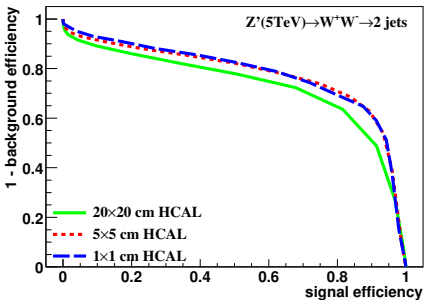

(a) 5 TeV rawhit cut at 0.25GeV

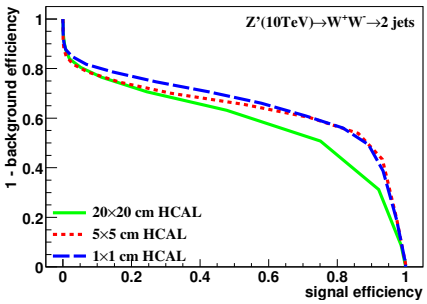

(b) 10 TeV rawhit cut at 0.25GeV

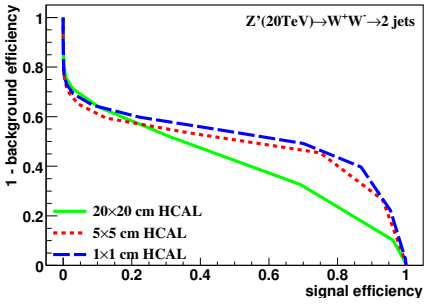

(c) 20TeV rawhit cut at 0.25GeV

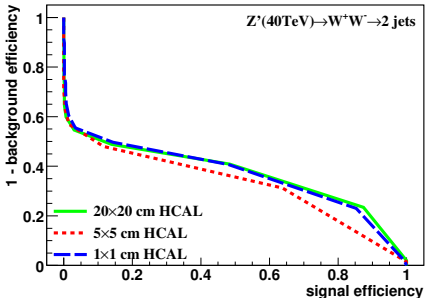

(d) 40 TeV rawhit cut at 0.25GeV

Figure 8: Signal efficiency versus background rejection rate using τ_{21}.The energies of collision at (a)5, (b)10, (c)20, (d)40TeV are shown here. In each picture, the three ROC curves correspond to different detector sizes.

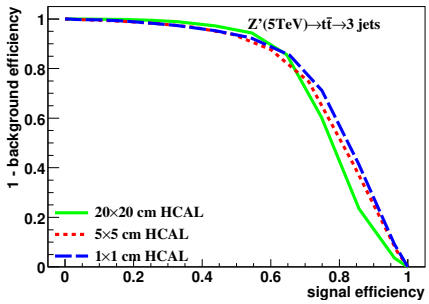

(a) 5 TeV rawhit cut at 0.25GeV

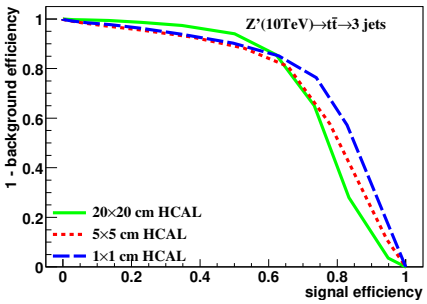

(b) 10 TeV rawhit cut at 0.25GeV

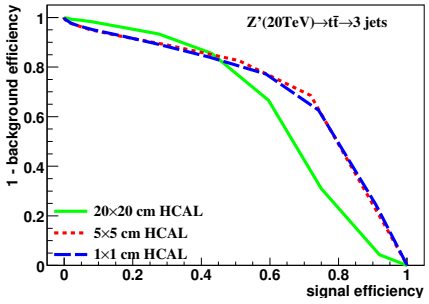

(c) 20 TeV rawhit cut at 0.25GeV

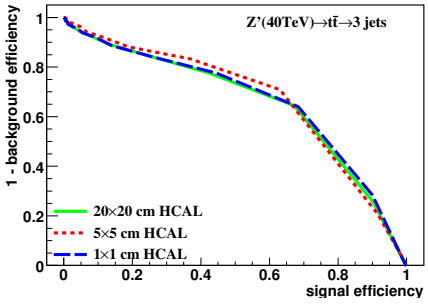

(d) 40 TeV rawhit cut at 0.25GeV

Figure 9: Signal efficiency versus background rejection rate using τ_{32}.The energies of collision at (a)5, (b)10, (c)20, (d)40TeV are shown here. In each picture, the three ROC curves correspond to different detector sizes.

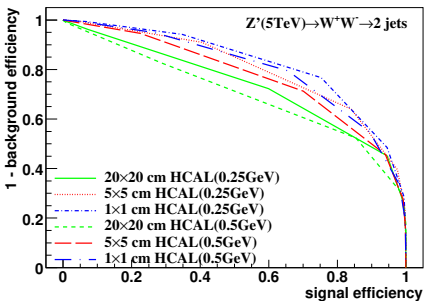

(a) 5 TeV rawhit cut 0.5GeV compare with cut 0.25GeV

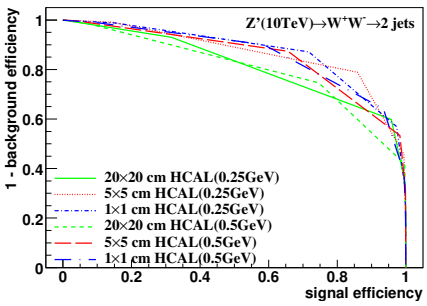

(b) 10 TeV rawhit cut 0.5GeV compare with cut 0.25GeV

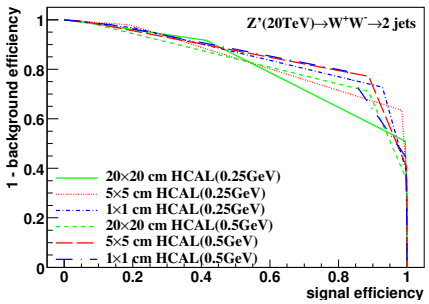

(c) 20 TeV rawhit cut 0.5GeV compare with cut 0.25GeV

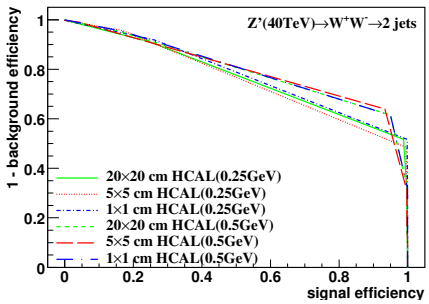

(d) 40 TeV rawhit cut 0.5GeV compare with cut 0.25GeV

Figure 10: Signal efficiency versus background rejection rate using $c_2^{(1)}$.The energies of collision at (a)5, (b)10, (c)20, (d)40TeV are shown here. In each picture, the six ROC curves correspond to different detector sizes in different cut.

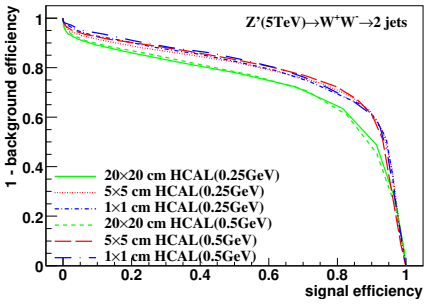

(a) 5 TeV rawhit cut 0.5GeV compare with cut 0.25GeV

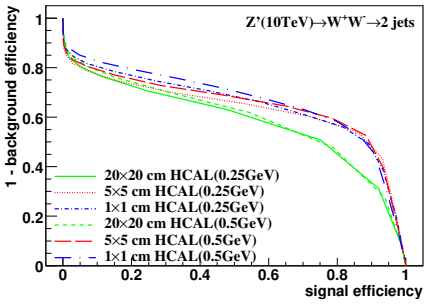

(b) 10 TeV rawhit cut 0.5GeV compare with cut 0.25GeV

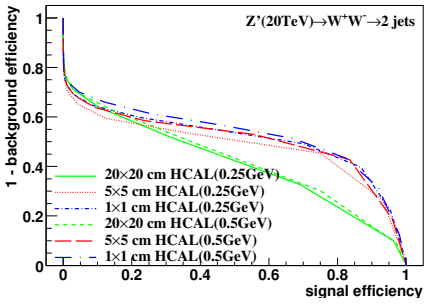

(c) 20TeV rawhit cut 0.5GeV compare with cut 0.25GeV

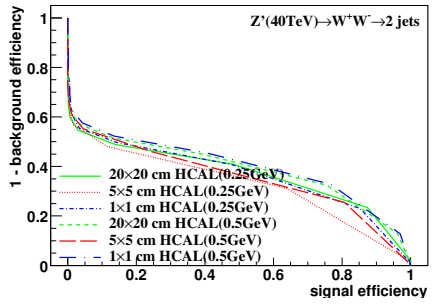

(d) 40 TeV rawhit cut 0.5GeV compare with cut 0.25GeV

Figure 11: Signal efficiency versus background rejection rate using τ_{21}.The energies of collision at (a)5, (b)10, (c)20, (d)40TeV are shown here. In each picture, the six ROC curves correspond to different detector sizes in different cut.

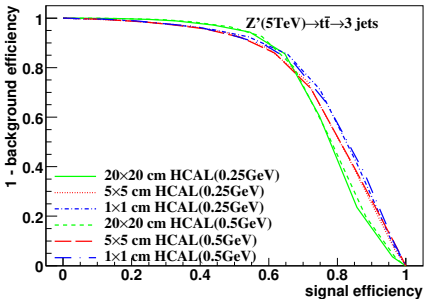

(a) 5 TeV rawhit cut 0.5GeV compare with cut 0.25GeV

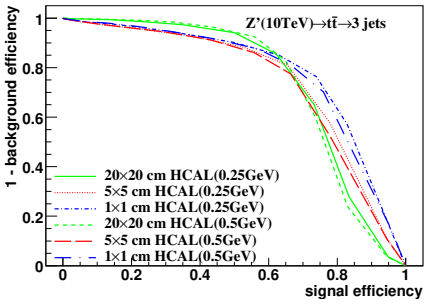

(b) 10 TeV rawhit cut 0.5GeV compare with cut 0.25GeV

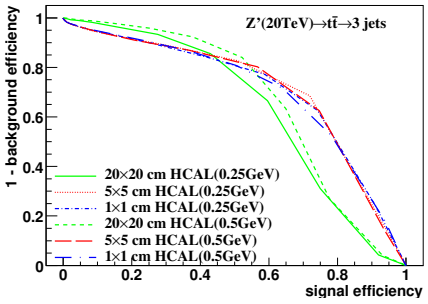

(c) 20 TeV rawhit cut 0.5GeV compare with cut 0.25GeV

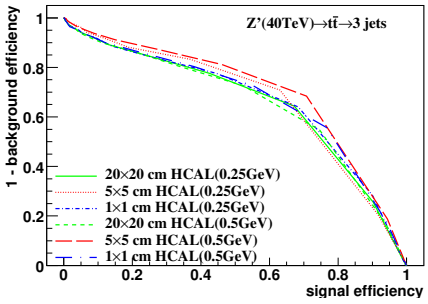

(d) 40 TeV rawhit cut 0.5GeV compare with cut 0.25GeV

Figure 12: Signal efficiency versus background rejection rate using τ_{32}.The energies of collision at (a)5, (b)10, (c)20, (d)40TeV are shown here. In each picture, the six ROC curves correspond to different detector sizes in different cut.